THE JOURNAL OF BIOLOGICAL CHEMISTRY
Vol. 277, No. 5, Issue of February 1, pp. 3793–3800, 2002

Printed in U.S.A.

Modulation of Mouse Paneth Cell α-Defensin Secretion by mIKCa1, a Ca^{2+}-activated, Intermediate Conductance Potassium Channel*

Received for publication, August 6, 2001, and in revised form, November 1, 2001
Published, JBC Papers in Press, November 27, 2001, DOI 10.1074/jbc.M107507200

Tokiyoshi Ayabe‡, Heike Wulff§, Dalila Darmoul¶, Michael D. Cahalan§, K. George Chandy§‖, and Andre J. Ouellette‡‖**

From the Departments of ‡Pathology, §Physiology and Biophysics, and ‖Microbiology and Molecular Genetics, College of Medicine, University of California, Irvine, California 92697-4800 and the ¶INSERM U 410, Faculté de Médecine Xavier Bichat, 75018 Paris, France

Paneth cells in small intestinal crypts secrete microbicidal α-defensins in response to bacteria and bacterial antigens (Ayabe, T., Satchell, D. P., Wilson, C. L., Parks, W. C., Selsted, M. E., and Ouellette, A. J. (2000) *Nat. Immunol.* 1, 113–138). We now report that the Ca^{2+}-activated K^+ channel mIKCa1 modulates mouse Paneth cell secretion. mIKCa1 cDNA clones identified in a mouse small intestinal crypt library by hybridization to human IKCa1 cDNA probes were isolated, and DNA sequence analysis showed that they were identical to mIKCa1 cDNAs isolated from erythroid cells and liver. The genomic organization was found to be conserved between mouse and human IKCa1 as shown by comparisons of the respective cDNA and genomic sequences. Reverse transcriptase-PCR experiments using nested primers amplified mIKCa1 from the lower half of bisected crypts and from single Paneth cells, but not from the upper half of bisected crypts, villus epithelium, or undifferentiated crypt epithelial cells, suggesting a lineage-specific role for mIKCa1 in mouse small bowel epithelium. The cloned mIKCa1 channel was calcium-activated and was blocked by ten structurally diverse peptide and nonpeptide inhibitors with potencies spanning 9 orders of magnitude and indistinguishable from that of the human homologue. Consistent with channel blockade, charybdotoxin, clotrimazole, and the highly selective IKCa1 inhibitors, TRAM-34 and TRAM-39, inhibited (~50%) Paneth cell secretion stimulated by bacteria or bacterial lipopolysaccharide, measured both as bactericidal activity and secreted cryptdin protein, but the inactive analog, TRAM-7, did not block secretion. These results demonstrate that mIKCa1 is modulator of Paneth cell α-defensin secretion and disclose an involvement in mucosal defense of the intestinal epithelium against ingested bacterial pathogens.

Gene-encoded antimicrobial peptides are evolutionarily conserved molecules that all known species elaborate as components of innate immunity (1). Generally containing fewer than 40 amino acids, these biochemically diverse peptides have secondary structures that range from linear α-helical molecules to β-sheet peptides constrained by up to four disulfide connectivities, including the covalently closed circular θ-defensins (2). In mammals, the α-defensins are cationic, 3–4-kDa peptides with a characteristic tridisulfide array, and they occur in phagocytic leukocyte granules from which they mediate nonoxidative killing of ingested microbial cells following phagolysosomal fusion (3–5). Varied epithelia also express α- and β-defensins, secreting them onto mucosal surfaces by apparent constitutive pathways or as secretory granule components of exocytotic cells (6–13). In crypts of the small intestinal epithelium, Paneth cells accumulate high levels of α-defensins that are termed cryptdins in mice, and which they secrete in response to bacterial or pharmacologic stimuli.

Paneth cells participate in innate mucosal immunity by discharging α-defensins at millimolar concentrations. Bacteria or bacterial antigens stimulate mouse Paneth cells to release apical secretory granules that contain several bactericidal peptides and proteins of which the cryptdins account for ~70% of the secreted microbicidal peptide activity (10). The secretory responses occur within minutes of exposure to soluble bacterial antigens or to carbamyl choline and are dose-dependent, suggesting a receptor-mediated process (10). In mouse small intestinal crypts stimulated with carbamyl choline, the cytosolic calcium dynamics change only in Paneth cells in a biphasic pattern consistent with mobilization of intracellular Ca^{2+} stores followed by influx of extracellular Ca^{2+} (14, 15). These observations led to the hypothesis that Paneth cell secretion in response to bacterial stimuli may be modulated by a cation-selective channel that could regulate the influx of extracellular Ca^{2+}.

Intermediate conductance Ca^{2+}-activated K^+ channels are the product of the IKCa1 genes (also known as IK1, hKCa4, hSK4, KCNN4) and are important in regulating the membrane potential of colonic epithelial cells, and lymphocytes, and in the volume regulation of red blood cells (16–20). IK_{Ca} channels have an intermediate single channel conductance of 11 picosiemens in sodium and 40 picosiemens in potassium Ringer, are voltage-independent, and open in response to changes in intracellular Ca^{2+}. The protein has six transmembrane segments, internal N and C termini, and its C terminus is complexed to calmodulin, the channel calcium sensor (21). The azole antimycotic, clotrimazole (CLT),[1] blocks this channel

* This work was supported by National Institutes of Health Grants DK44632 (to A. J. O), MH59222 (to K. G. C.), and NS14609 (to M. D. C.) and by Western States Affiliate of the American Heart Association Award 9920014Y (to H. W.). The costs of publication of this article were defrayed in part by the payment of page charges. This article must therefore be hereby marked "*advertisement*" in accordance with 18 U.S.C. Section 1734 solely to indicate this fact.

** To whom correspondence should be addressed: Dept. of Pathology, College of Medicine, University of California, D-440, Medical Science 1, Irvine, CA 92697-4800. Tel.: 949-824-4647; Fax: 949-824-1098; E-mail: aouellet@uci.edu.

[1] The abbreviations used are: CLT, clotrimazole; ChTX, charybdotoxin; K_{Ca}, calcium-activated K^+ channel; IK_{Ca}, intermediate conductance K_{Ca}; LPS, lipopolysaccharide; NCR, noncoding region; RT, reverse transcriptase; TRAM, triarylmethane; TRAM-3, (2-chlorophenyl)diphenylmethanol; TRAM-7, 1-tritylpyrroline; TRAM-34, 1-[(2-chlorophenyl) diphenylmethyl]-1*H*-pyrazole; TRAM-39, 2-(2-chlorophenyl)-2,2-diphenylacetonitrile; PIPES, 1,4-piperazinediethanesulfonic acid; cfu, colony-stimulating unit(s).

with nanomolar affinity, and triarylmethane analogs of CLT are highly selective and potent inhibitors of the human IKCa1 channel (22). Scorpion toxin charybdotoxin (ChTX) also blocks hIKCa1, and a selective analog, ChTx-Glu^{32}, has been generated by structure-guided design (23). These highly selective reagents provide probes for analyzing the role of IKCa1 in Ca^{2+}-mediated signaling events.

Because hIKCa1 regulates specific immune responses mediated by T lymphocytes (20, 24), we tested whether a K_{Ca} channel could participate in innate immune responses to bacteria by modulating calcium signaling during Paneth cell secretion. In this report, mouse Paneth cells in small intestinal epithelium are shown to express mIKCa1, and pharmacologic inhibition of IKCa1 with highly selective triarylmethanes (22) diminished cryptdin secretion in response to bacteria and lipopolysaccharide (LPS).

EXPERIMENTAL PROCEDURES

Preparation of a Mouse Small Intestinal Crypt cDNA Library—Crypts from the small intestines of adult Swiss Webster mice were prepared using EDTA dissociation (10, 25–27). Fractions consisting of >90% crypts were obtained by agitation of small intestinal segments in nominally Ca^{2+}, Mg^{2+}-free phosphate-buffered saline with 30 mM EDTA. Total crypt cellular RNA was isolated (28, 29), from which poly(A)-containing mRNA was purified by oligo(dT)-cellulose chromatography. A custom cDNA library was constructed by Stratagene Cloning Systems, Inc. (La Jolla, CA) using crypt mRNA as template for reverse transcription of single-stranded cDNA with oligo$(dT)_{18-20}$ to prime the reverse transcriptase reaction from the mRNA 3′ termini. Double-stranded cDNAs with adapted termini were cloned in the *Eco*RI and *Xho*I sites of the phagemid vector Uni-ZAP XR (Stratagene Cloning Systems). Cloning was performed without polymerase chain reaction (PCR) amplification of sequences or size exclusion of low molecular weight mRNAs. The library contained $\sim 9.8 \times 10^6$ primary clones and was amplified to a working titer of 3.9×10^{10} plaque-forming units/ml.

Cloning of Mouse Crypt mIKCa1 cDNA—Bacteriophages containing mIKCa1 were identified in the crypt library by screening $\sim 5 \times 10^6$ plaque-forming units in duplicate by hybridization at 42 °C in 1 M NaCl, 50% formamide, 10% dextran sulfate, and 1% SDS with ^{32}P-labeled probes consisting of 360 bp from the 5′-NCR of hIKCa1 (GenBank™ accession number AF033021). Filters were washed three times with continuous agitation at 50 °C with 0.5 × SSC (1 × SSC = 150 mM NaCl, 15 mM sodium citrate), 1% SDS, and autoradiograms were exposed at −70 °C. Forty-six positive clones were identified, shown to have identical or overlapping restriction patterns, and all clones sequenced within the IKCa1 coding region were identical to mIKCa1. Plaque-purified phage were excised to plasmid forms and subjected to digestion with restriction enzymes and DNA sequence analysis. All clones corresponded to the mouse Ca^{2+}-activated K^+ channel, mIKCa1. The complete mouse intestinal *mIKCa1* sequence was determined by cloning the remaining 5′-flanking by 5′-rapid amplification of cDNA ends using oligonucleotide primers mCK1m1, 5′-ATGGC CCCTG AGGTC TTGGG GCTCA GCCAG CTT (nucleotides 145–177 on the mIKCa1 antisense strand); mCK1m2, 5′-TGCCC AGGGT CCCCC ACCTC TCAGT ACTGC AAAT (nucleotides 109–142 on the mIKCa1 antisense strand), and mCK1mR, 5′-TTCTC CTGCT CCAGC AGGCG CTTTC TCCGT CTCA (nucleotides 210–243 on the mIKCa1 antisense strand) as primers in the 5′-rapid amplification of cDNA ends System Version 2.0 (Invitrogen). The complete mouse intestinal crypt mIKCa1 cDNA sequence was identical to those reported previously from mouse bone marrow (GenBank™ accession numbers AF042487 and NM008433) and embryonic mouse liver (GenBank™ accession number AK010943).

RT-PCR Detection of mIKCa1 mRNA—Intact crypts and villi were prepared as described previously (10). Crypts were bisected by suspending crypt preparations at low density in 0.6% agarose in PBS at 50 °C, poured onto the surface of a microscope slide, and allowed to solidify. Individual crypts were bisected under phase microscopy using pulled capillary pipettes that were broken to produce knife edges. For preparation and isolation of single Paneth cells, crypt preparations were incubated in 2 ml of Hanks' balanced salt solution with 150 units/ml collagenase (Sigma) at 37 °C for 15 min. Cells were deposited by centrifugation at 1500 rpm for 5 min in a Beckman GS-6R centrifuge, resuspended, and washed two times with ice-cold PBS, and the preparation was centrifuged through a 30-μm filter Cell Strainer cap (Falcon model 352235). Paneth cells and agranular crypt epithelial cells were identified under phase microscopy, drawn into capillary tubes and transferred to PCR reaction tubes for amplification.

For RT-PCR experiments, isolated villi, intact crypts, bisected crypts, or isolated single Paneth cells were transferred to individual microcentrifuge tubes, sonicated in 1 μl of RNAguard RNase inhibitor, and stored at −70 °C. Detection of mIKCa1 required that RT-PCR be performed with nested primer sets. RNA from intestinal epithelial cells and structures were amplified with GeneAmp EZ r*Tth* RNA PCR kit (PerkinElmer Life Sciences). Samples (500 ng) of total RNA from mouse bone marrow, spleen, liver, kidney, testis, heart, stomach, small intestine (proximal, mid, distal), cecum, colon, and developing small intestine also were analyzed similarly (data not shown). The external amplimers consisted of primers mIKCa1F1, 5′-GCCAG GTACG GCTGA AACAC, which corresponds to nucleotides 1224–1244 on the mIKCa1 sense strand within exon 7 and mIKCa1R1, 5′-CGTGG GAGGT CCAAT TCAGT, which corresponds to nucleotides 1624–1643 on the mIKCa1 antisense strand in exon 8. Reaction mixes were denatured and subjected to 45 cycles as follows: 94 °C, 1 min; 50 °C, 1.5 min; 72 °C, 2 min with a final extension reaction of 9 min at 72 °C terminated by rapid cooling to 4 °C.

Detection of mIKCa1 required an additional round of amplification using the following set of internal amplimers: mIKCa1F2, 5′-ACATG ATCCT GTGCG ACCTG corresponding to nucleotides 1293–1312 on the mIKCa1 sense strand and also in exon 7 paired with mIKCa1R2, 5′-TCAAC GTGGA TCCAC GTGGG corresponding to nucleotides 1567–1586 on the mIKCa1 antisense strand in exon 8. Samples consisting of 5 μl of 1:100 dilutions of the initial RT-PCR reaction products were used as template for nested amplification. PCR mixes lacking AmpliTaq DNA Polymerase were preheated at 94 °C for 2 min, then complete reaction mixes were cycled as before. Samples of the PCR reactions were analyzed by separation in 2% agarose gels to visualize the 293-bp product, and the fragments were purified with QIAEX II gel extraction kit (Qiagen, Valencia, CA) or transferred to nylon membranes to identify mIKCa1 by hybridization with an hIKCa1 probe (29, 30). Amplification of mIKCa1 was performed a minimum of four times on unstained, freshly prepared crypts. The 293-bp amplification product was cloned into the TOPO II TA cloning vector (Invitrogen), and its identity as the appropriate region of mIKCa1 sequence was confirmed by DNA sequencing (data not shown).

Inhibition of Paneth Cell Secretion by mIKCa1-specific Blockers—To test for a role for *mIKCa1* in Paneth cell secretion, the inhibitory effects of K^+ channel blockers were tested in an *ex vivo* crypt assay system as described previously (10, 27). One-thousand crypts were incubated in 1 ml of isotonic PIPES buffer, consisting of 10 mM PIPES with 0.8% sodium gluconate (pH 7.4), with the appropriate inhibitor plus 10^6 colony-forming units (cfu) *Salmonella typhimurium*, *Escherichia coli*, or *E. coli* LPS (Sigma) or in buffer alone at 37 °C for 30 min. Samples of elicited secretions were collected and analyzed for bactericidal activity and in Western blots for cryptdins. Samples (10 μl) of collected secretions or control supernatants were tested for bactericidal activity against 1,000 cfu of the defensin-sensitive *S. typhimurium phoP*− strain in 40 μl of PIPES buffer, and surviving bacteria were quantitated as cfu on nutrient agar after overnight growth at 37 °C (10). In this assay, ~1000 crypts were suspended in 1 ml of a nominally calcium-free medium (10 mM PIPES, 0.8% sodium gluconate (pH 7.4)) and exposed to 1×10^6 bacterial cfu per crypt or to 100 ng/ml *E. coli* LPS to elicit Paneth cell secretion (10). All experiments were repeated a minumum of three times on freshly prepared crypts.

Western Blot Analysis—Proteins extracted from collected secretions were analyzed for cryptdins by Western blotting following separation by acid-urea PAGE. Briefly, the samples were analyzed on a 12.5% acrylamide acid-urea PAGE gel containing 5 M urea as described previously (10). For Western blot analysis, resolved Paneth cell protein secretions were transferred from gels to nitrocellulose membranes (0.22 μm), and blocked membranes were incubated sequentially with rabbit anti-mouse cryptdin-1 antibody (1:500), peroxidase-conjugated anti-rabbit IgG (1:10,000), and chemiluminescent substrate (SuperSignal, Pierce), and x-ray films were exposed to blots as described previously (10).

Electrophysiology of mIKCa1—The mIKCa1 coding region was cloned into pcDNA 3.1, and the construct was transiently transfected into COS-7 cells with FuGENE 6 (Roche Molecular Biochemicals) according to the manufacturer's protocol. The pharmacology of mIKCa1 was determined in the whole cell mode of the patch-clamp technique using a holding potential of −80 mV. A pipette solution containing 145 mM K^+ aspartate, 10 mM K_2EGTA, 8.5 mM $CaCl_2$, 2.0 mM $MgCl_2$, and 10 mM HEPES (pH 7.2, 290–310 mosM), with a calculated free $[Ca^{2+}]_i$ of 1 μM was used to activate mIKCa1. To eliminate native COS cell chloride currents, sodium aspartate Ringer solution (160 mM Na^+ aspartate, 4.5

mM KCl, 2 mM $CaCl_2$, 1 mM $MgCl_2$, 5 mM HEPES (pH 7.4), 290–310 mosM) was used as an external solution. Currents were elicited by 200-ms voltage ramps from −120 to 40 mV every 10 s, and the reduction of slope conductance at −80 mV by channel antagonists were taken as a measure of channel blocking. The recording in Fig. 3*A* was done on excised inside-out patches with the external solution described above as pipette solution. K^+ aspartate solutions containing 1 μM and 50 nM free [Ca^{2+}] were applied to the cytoplasmic side of the patch. CLT, econazole, and tetraethylammonium were from Sigma; nifedipine was from RBI (Natick, MA); ChTX, ChTX-Glu[32], and ShK (*Stichodactyla helianthus* toxin) were from Bachem Biosciences (King of Prussia, PA). The synthesis and specificities of ChTX-Glu[32] (23) and the triarylmethanes TRAM-3, TRAM-7, TRAM-34, and TRAM-39 have been described previously (22).

RESULTS

Cloning of mIKCa1 cDNA from Adult Mouse Small Intestinal Crypts—A cDNA library prepared from isolated adult mouse small intestinal crypts was screened in duplicate with a probe from the 5′-NCR of hIKCa1 (GenBank™ accession number AF033021). Forty-six positive clones with identical or overlapping restriction patterns were identified in the mouse crypt library. The complete 1278-bp coding sequence was obtained in several isolates, but the remaining 175 bp of 5′-NCR was determined by 5′-rapid amplification of cDNA ends. The composite mIKCa1 sequence contains 302 bp of 5′-NCR, 1278 bp of coding sequence, and 496 bp of 3′-NCR. The sequence is identical to amplified mIKCa1 coding regions from the MEL murine erythroleukemia cell line characterized previously (GenBankTM accession numbers AF042487, AF072884, and NM_008433) and with full-length mIKCa1 cDNA from mouse embryonic liver (GenBankTM accession number AK010943). mIKCa1 cDNA alignments with existing mouse genomic DNA sequences (GenBankTM accession numbers AC073693 and AC073810) showed that the intron-exon organization of the mIKCa1 gene is identical to that in the hIKCa1 homologue (Fig. 1). Comparison of the hIKCa1 cDNA and genomic sequences (GenBankTM accession numbers AF022797 and AF305731–AF305735) with mIKCa1 sequences revealed >90% nucleotide sequence identity from nucleotide 97 of the human transcript through the coding region and 3′-NCR. The hIKCa1 coding region is 6 nucleotides longer than mIKCa1, coding for two additional residues in the S3-S4 loop. The deduced mIKCa1 protein differs from hIKCa1 at 53 additional positions, most differences being in the S2 and S3 segments, and in the C terminus. These cloning results show that mIKCa1 is expressed by mouse small intestinal crypt epithelium.

mIKCa1 mRNA Is Expressed Selectively in Paneth Cells in the Mouse Small Intestine—The intestinal epithelial cell lineages that express the mIKCa1 gene in mouse small intestinal epithelium were determined using a nested RT-PCR assay. Consistent with previous reports (18, 20), RT-PCR analysis of whole organ RNA showed that mIKCa1 mRNA was present in adult mouse bone marrow, spleen, liver, kidney, testis, heart, stomach, small intestine, cecum, and colon (data not shown). Also, mIKCa1 mRNA was amplified equivalently from whole organ RNA throughout the gastrointestinal tract, and its detection in neonatal mouse small bowel RNA (not shown) showed that mIKCa1 gene expression precedes crypt ontogeny and the differentiation of epithelial cell lineages. Because amplification of whole organ RNA provides no information as to sites of gene expression, we attempted to determine the cell types expressing mIKCa1 mRNA in small bowel by *in situ* hybridization. However, mIKCa1 mRNA levels were insufficient to detect hybridization, and therefore small intestinal mIKCa1 expression was investigated by the RT-PCR analysis of isolated epithelial structures and cells.

In mice, Paneth cells were the primary small intestinal epithelial cell lineage found to express mIKCa1. To identify the small intestinal cell types expressing mIKCa1, nested RT-PCR assays were performed on isolated intact villus epithelium (Fig. 2*A*, "*arrow a*"), intact crypts (Fig. 2*A*, "*arrow b*"), bisected crypts (Fig. 2*A*, "*arrows c* and *d*"), single Paneth cells (Fig. 2*A*, "*arrows g* and *h*"), or single undifferentiated crypt cells (Fig. 2*A*, "arrows *i* and *j*"). Individual structures or cells were transferred to separate microfuge tubes, mIKCa1 cDNA was amplified using sequence-specific nested amplimers, and the products were analyzed by gel electrophoresis (see "Experimental Procedures"). mIKCa1 mRNA was detected in intact crypts (Fig. 2*B*, *lane b*) but not in villus epithelium (Fig. 2*B*, *lane a*), and analyses of bisected crypts showed that mIKCa1 mRNA was present only in the lower portion of the crypt (Fig. 2*B*, *lane d*) but not in the upper half (Fig. 2*B*, *lane c*). Since the lower half of the crypt contains Paneth cells as well as undifferentiated crypt epithelial cells that are agranular, RT-PCR assays were conducted on both these cell populations isolated from single cell suspensions of isolated crypts (see "Experimental Procedures"). Although Fig. 2 shows Paneth cells in crypts stained selectively with Amido Black (see "Experimental Procedures"), all RT-PCR experiments reported here were performed on unstained crypts and are representative of four separate determinations. Single cell RT-PCR detected mIKCa1 mRNA only in Paneth cells (Fig. 2*B*, *lanes g* and *h*, respectively, containing one or five individual Paneth cells), but not in agranular crypt epithelial cells (Fig. 2*B*, *lanes i* and *j*, one or five cells, respectively). Glyceraldehyde-3-phosphate dehydrogenase mRNA was amplified using RNA from all sources in Fig. 2 that were negative for mIKCa1 products (data not shown). Hybridization of a mIKCa1 cDNA probe to a Southern blot of the gel shown in the *upper panel* of Fig. 2*B* was consistent with identification of the amplification products as mIKCa1 sequences (Fig. 2*B*, *lower panel*). The authenticity of the amplified products was verified by DNA sequence analysis (data not shown).

mIKCa1 and hIKCa1 Are Pharmacologically Indistinguishable—Because mouse and human IKCa1 differ at 55 amino acid residue positions (13% difference), we compared the properties of the mouse channel heterologously expressed in COS-7 cells with that of human IKCa1. In the representative inside-out patch shown in Fig. 3*A*, mIKCa1 currents were induced by 1 μM free Ca^{2+}, but not by 50 nM Ca^{2+}, confirming the Ca^{2+} dependence of this channel. In experiments done in the whole cell mode, the reversal potential of the mIKCa1 current shifted from −80 mV in sodium Ringer solution to 0 mV in potassium Ringer, consistent with the channel being potassium-selective (Fig. 3*B*). We also conducted a detailed pharmacological analysis of mIKCa1 using a panel of ten inhibitors that are known to block hIKCa1 in a potency range spanning 9 log units (20, 21). Representative traces for four compounds (TRAM-34, ChTX-Glu[32], CLT, and TRAM-7) are shown in Fig. 3, *C–F*, and dose-response curves for all ten compounds are shown in detail in Fig. 3*G*. The K_d-values (mean + S.D.) obtained for the mouse channel are identical to those reported for the human homologue, hIKCa1 (20, 21). Earlier published data demonstrated that the single channel conductances of mIKCa1 and hIKCa1 are identical (17, 18). Taken together, these findings show that the biophysical and pharmacological properties of the mIKCa1 channel are indistinguishable from those of hIKCa1, allowing the previously characterized and selective inhibitors of hIKCa1, TRAM-34, TRAM-39, and ChTX-Glu[32] to be applied to functional studies of mIKCa1 in Paneth cells.

mIKCa1 Blockers Suppress Paneth Cell Secretory Responses to Bacteria and LPS—The selective expression of mIKCa1 in Paneth cells of mouse small intestinal epithelium suggested that mIKCa1 may regulate Ca^{2+}-mediated events in Paneth cell secretion (15). To test this concept, the effects of mIKCa1

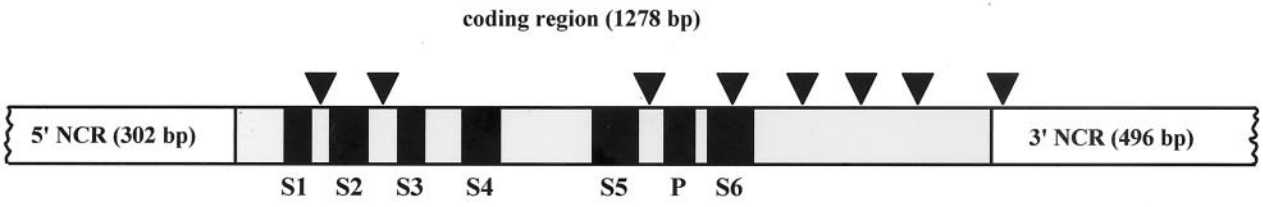

	Donor	Intron	Acceptor
	GlyCysLys	I	TrpValLeu
mouse cDNA	GGCTGCAAG		TGGGTGCTG
mouse gen:	GGCTGCAAGgtgagtgg		cccccacagTGGGTGCTG
human gen:	GGGTGCTCGgtgagtgg		ccctgacagTGGGCGCTC
	GlyCysSer		TrpAlaLeu
	GluValGln	II	LeuPheMet
mouse cDNA	GAGGTCCAG		CTGTTGATG
mouse gen:	GAGGTCCAGgtaagctg		tccctgcagCTGTTGATG
human gen:	GAGGTCCAGgtagggtg		taccggcagCTGTTCATG
	GluValGln		LeuPheMet
	AlaGluAr	III	gGlnAlaVal
mouse cDNA	GCTGAGAG		GCAGGCTGTC
mouse gen:	GCTGAGAGgtgaggg		cccatagGCAGGCTGTC
human gen:	GCCGAGAGgtagggtg		cccatagGCAGGCTGTT
	AlaGluAr		gGlnAlaVal
			===S6===
	GlyValMet	IV	GlyValCys
mouse cDNA	GGAGTCATG		GGGGTCTGC
mouse gen:	GGAGTCATGgtgagtac		cccacagGGGGTGTGC
human gen:	GGAGTCATGgtgagtac		cccacagGGTGTCTGC
	GlyValMet		GlyValCys
	AlaLysGlu	V	MetLysGlu
mouse cDNA:	GCCAAAGAG		ATGAAGGAG
mouse gen:	GCCAAAGAGgtgaggct		cccgtcagATGAAGGAG
human gen:	ACCAAAGAGgtgagatg		acccccagATGAAGGAG
	ThrLysGlu		MetLysGlu
	IleHisTh	VI	rPheArgGln
mouse cDNA:	ATCCACAC		GTTCCGCCAG
mouse gen:	ATCCACACgtgagggcctgggtg		ccccacagGTTCCGCCAG
human gen:	ATCAACGCgtgagggcc		tcccacagGTTCCGCCAG
	IleAsnAl		aPheArgGln
	IleSerLys	VII	MetHisMet
mouse cDNA:	ATCTCCAAG		ATCCACATG
mouse gen:	ATCTCCAAGgtaccagg		ccacccagATGCACATG
human gen:	ATCTCCAAGgtactagg		ccacccagATGCACATG
	IleSerLys		MetHisMet
	AlaThr *	VIII	
mouse gen:	GCCACATAGCTCCACATGgtgagtggg		cttctcagAACTCACAG

FIG. 1. **Comparison of genomic organization and intron-exon junctions of mouse and human IKCa1.** The putative transmembrane segments (S1–S6) in the coding region, the 5′- and 3′-NCR, and the intron-exon junctions (*arrowheads*) are depicted in the schematic at the *top* of the figure. Donor and acceptor splice site sequences at each of the conserved exon-intron boundaries between mIKCa1 and hIKCa1 are shown below. Consensus GT-AG (5′-3′) splice site sequences are observed at each junction.

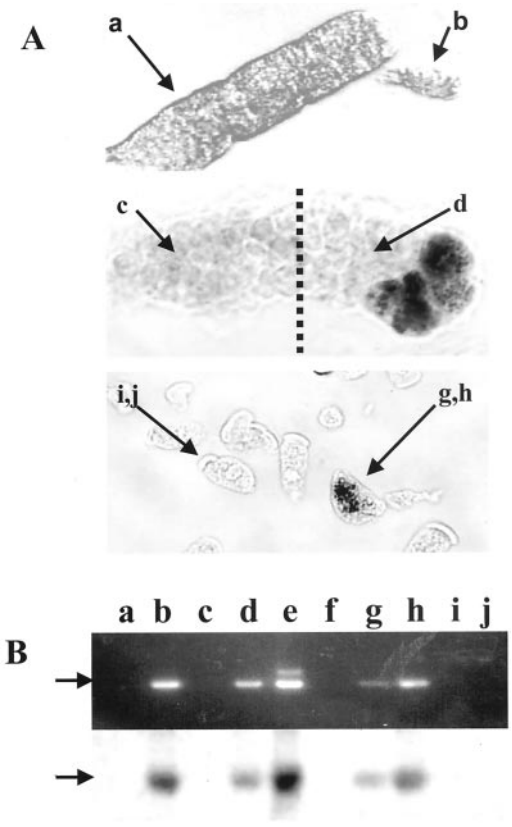

FIG. 2. **mIKCa1 mRNA in mouse Paneth cells.** Crypts, villi, and crypt cell preparations are described under "Experimental Procedures." *A*, individual isolated villi (*arrow a*), intact crypts (*arrow b*), crypts bisected as shown (*arrows c* and *d*), single Paneth cells (*arrows g* and *h*), and agranular crypt epithelial cells (*arrows i* and *j*) are shown under phase microscopy. In the center and lower panels, epithelia and cells are shown after staining 2 min with 0.05% Amido Black, a selective Paneth cell stain under these conditions, but all RT-PCR amplifications were performed on unstained preparations. mIKCa1 sequences in individual, unstained isolated villi (*arrow a*), intact crypts (*arrow b*), upper (*arrow c*) and lower (*arrow d*) portions of bisected crypts, one or five isolated Paneth cells (*arrows g* and *h*, respectively), or one or five isolated agranular crypt epithelial cells (*arrows i* and *j*) are shown. *B,* lanes labeled *a–d* and *g–j* correspond to samples of nested mIKCa1 products amplified from cells and structures as denoted in *A*. *Lane e* contains mIKCa1 products amplified from 500 ng of total adult mouse small bowel RNA; and *lane f* contains a sample from an identical reaction to which no template RNA had been added. The lower half of *B* shows an autoradiogram of a Southern blot of the gel in the upper half after hybridization with an mIKCa1 cDNA probe. *Arrows* denote the position of the mIKCa1-specific product.

channel blockers were tested as inhibitors of Paneth cell α-defensin secretion following exposure to *S. typhimurium* or *E. coli* or to 100 ng/ml LPS for 30 min (10). Because cryptdins localize exclusively to Paneth cell secretory granules in the small intestine and account for 70% of the bactericidal activity in Paneth cell secretions (10), bactericidal peptide activity assays provide a sensitive and accurate index of Paneth cell secretion. Accordingly, the effects of IKCa1 blockers on secretory activity were evaluated by measuring antimicrobial peptide activity in elicited secretions, and cryptdin secretion was confirmed biochemically by Western blot analyses.

In the presence of 1 μM ChTX-Glu^{32} or CLT, the quantity of bactericidal activity secreted by Paneth cells in crypts exposed to *S. typhimurium* was inhibited by ~50% compared with crypts not exposed to blockers (Fig. 4*A*). Further studies with CLT showed that the inhibition was dose-dependent (Fig. 4*B*), and similar results were obtained with crypts exposed to 1000 cfu/crypt *E. coli* (data not shown). Although these findings were consistent with the involvement of mIKCa1 in Paneth cell secretory responses to bacteria, we perceived the need to test additional inhibitory agents with greater specificities. For example, ChTX, an agent used in preliminary experiments (Fig. 4*C* and data not shown) also blocks the BK_{Ca}, Kv1.2, and Kv1.3 channels (31), and CLT inhibits cytochrome P450-dependent enzymes (32–34) in the concentration range that blocks mIKCa1 (Fig. 3). Therefore, to test for mIKCa1 involvement in Paneth cell secretion of bactericidal peptide activity more specifically, the inhibitory effects of more selective mIKCa1 blockers were evaluated. As shown in Fig. 4, *A* and *C*, ChTX-Glu^{32}, selective for IKCa1 over Kv1.2 and Kv1.3 (23) (Fig. 3), inhibited bacterial and LPS-stimulated secretion of bactericidal peptide activity to the same extent as ChTX (Fig. 4*C*). The highly selective IKCa1 blockers TRAM-34 and TRAM-39 also inhibited LPS-triggered Paneth cell release of bactericidal peptide activity at 200 nM, nearly equivalent to the level of inhibition obtained using 1 μM CLT. On the other hand, the inactive analog TRAM-7 had no measurable inhibitory effect on secretion (Fig. 4*C*). None of the inhibitors was inherently bactericidal, and none stimulated Paneth cells to release granules (data not shown). These findings implicate the mIKCa1 channel as a specific modulator of Paneth cell α-defensin release in response to bacteria or LPS.

To evaluate the effects of mIKCa1 blockers on cryptdin secretion, Paneth cell secretions collected from crypts exposed to bacteria (Fig. 4, *A* and *B*) or LPS (Fig. 4*C*) were dialyzed, separated by acid-urea PAGE, and probed in Western blots with anti-cryptdin-1 antibody (Fig. 5). As reported previously (10), *S. typhimurium* evoked secretion of activated cryptdins (Fig. 5, *A* and *B*, *lanes 1*), and no measurable cryptdin was released when crypts were incubated for 30 min in isotonic buffer without stimuli (Fig. 5*A*, *lane 4*; Fig. 5*B*, *lane 5*). Consistent with the inhibitory effects of ChTX-Glu^{32} and CLT on release of bactericidal peptide activity (Fig. 4, *A* and *B*), 1 μM ChTX-Glu^{32} or 1 μM CLT reduced cryptdin-specific immunoreactivity in Paneth cell secretions elicited by bacteria (Fig. 5*A*), and this effect was dose-dependent (Fig. 5*B*). CLT (1 μM) and the specific IKCa1 inhibitors TRAM-34 and TRAM-39 (200 nM) also diminished LPS-induced cryptdin release from Paneth cells (Fig. 5*C*). These findings and those in Fig. 4 provide evidence that mIKCa1 has a role in Paneth cell secretion in response to infectious challenge, disclosing potential implications for innate immunity in small intestinal crypts exposed to bacteria.

DISCUSSION

From evidence of their secretion of cryptdins in response to bacteria and bacterial antigens, Paneth cells are inferred to participate in innate immunity in the crypt microenvironment and perhaps above the crypt-villus junction as well (10, 27). The highly restricted expression of mIKCa1 in Paneth cells of the small bowel, and the inhibition of bacterial stimulated Paneth cell secretion by highly selective mIKCa1 blockers, identify mIKCa1 as a functional marker for Paneth cells. Other intestinal cells may express mIKCa1 at levels below the detection limits of our assays.

Carbamyl choline-induced Paneth cell secretion is associated with a biphasic increase in cytosolic [Ca^{2+}], where the first rise in Ca^{2+} derives from intracellular stores and the second is dependent on uptake of exogenous Ca^{2+} (15). The involvement of the Ca^{2+}-activated mIKCa1 channel in Paneth cell secretory responses to bacteria and LPS suggests a role for cytosolic [Ca^{2+}] in this process as well. By analogy to events in human lymphocytes during the specific immune response, mIKCa1 channels in the Paneth cell membrane would open as cytosolic [Ca^{2+}] approaches 300 nM, providing the counterbalancing cation efflux necessary to sustain Ca^{2+} entry from the external

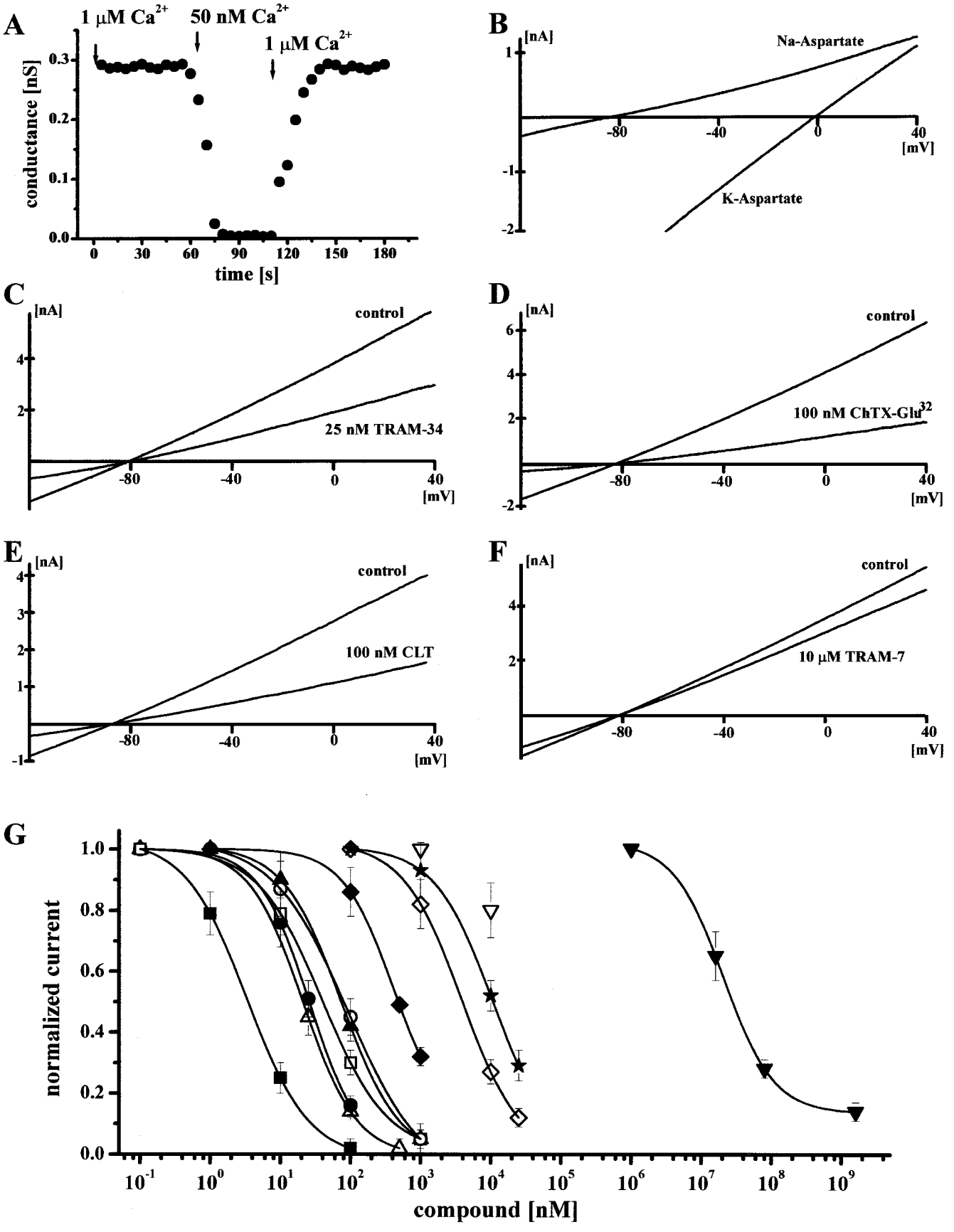

FIG. 3. **Electrophysiological properties of mIKCa1 expressed in COS-7 cells.** *A*, representative IK conductance in a single excised inside-out patch in the presence of 1 μM and 50 nM free [Ca^{2+}], demonstrating the calcium dependence of the current. This experiment was repeated on five additional patches. *B*, representative IK current recorded in the whole-cell mode in a COS-7 cell transfected with mIKCa1. In this experiment, the bath solution was changed from 160 mM sodium aspartate to 160 mM potassium, and the shift in reversal potential from −80 mV to 0 mV demonstrated the potassium selectivity of the current. This experiment was repeated on 10 additional cells. *C–F*, inhibitory effects of 25

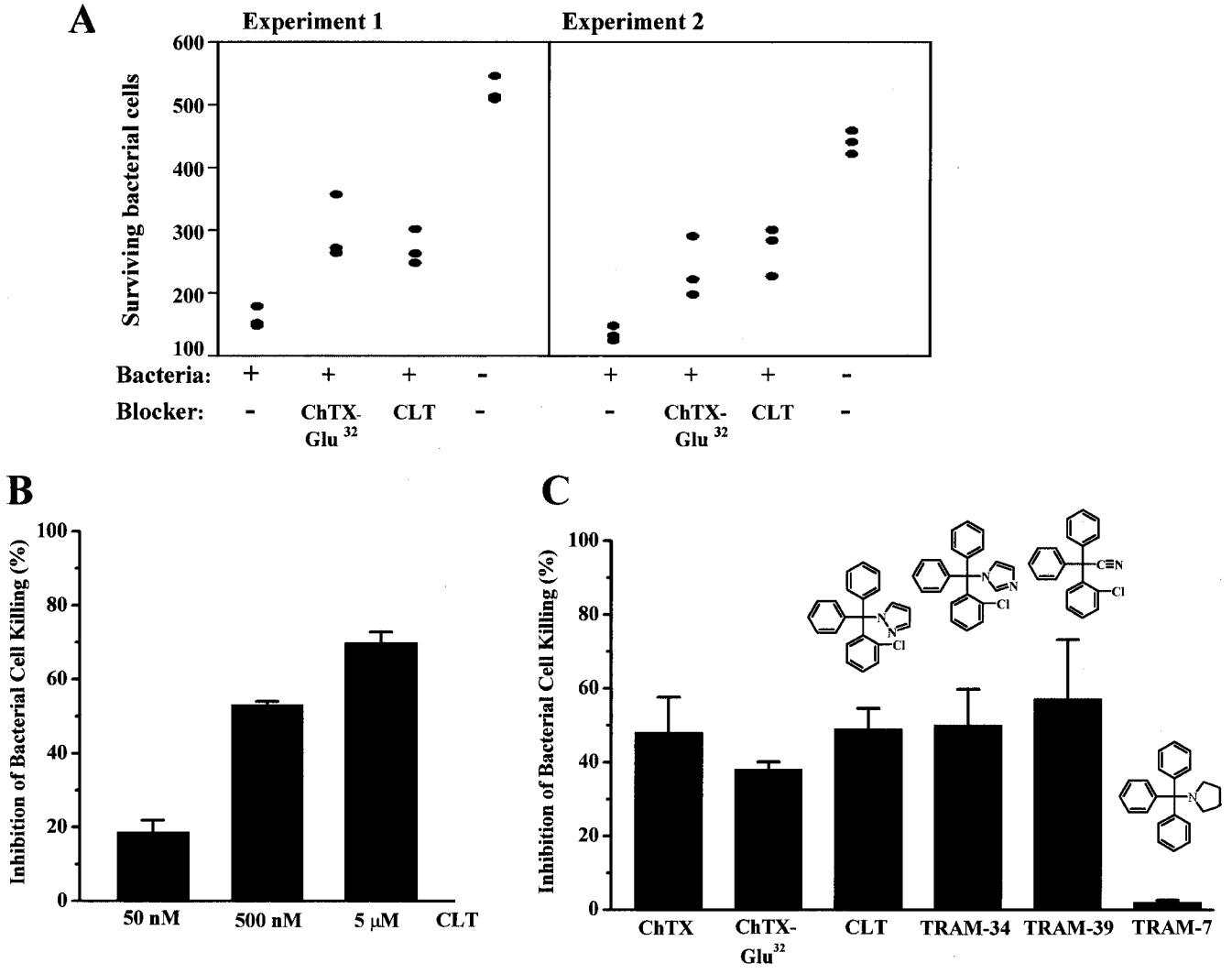

FIG. 4. **Effects of mIKCa1 inhibition on Paneth cell secretion of bactericidal peptide activity.** *A,* secretions were collected from crypts (~1000) resuspended in isotonic sodium gluconate buffer containing 1 μM CLT or 1 μM ChTX-Glu^{32} coincubated with *S. typhimurium* at 37 °C for 30 min. Stimulated secretions or control supernatants were collected, and the bactericidal activity of 10-μl samples were tested against ~500 cfu of defensin-sensitive *S. typhimurium* (10). Surviving bacteria were quantitated as colony-forming units following overnight growth. Data points represent individual triplicate determinations in two separate experiments. For each series of data points, *plus characters* denote presence of *S. typhimurium* with crypts as bacterial secretory stimuli, and *minus signs* denote crypts incubated in the absence of bacteria as negative controls for secretion. Similarly, CLT or ChTX-Glu^{32} blocking agents were present as noted, and *minus signs* denote crypts incubated in the absence of either blocker. *B,* secretions were collected from crypts stimulated with *S. typhimurium* in the presence of increasing concentrations of CLT, and the bactericidal activity of 10-μl samples of secretions was assayed as described in *A* and expressed as mean percent inhibition of bacterial cell killing ± S.D. (n = 3), relative to secretions stimulated by *S. typhimurium* in the absence of blocking agent. *C,* secretions were collected from crypts stimulated with 100 ng/ml LPS in the presence or absence of 200 nM TRAM-34, TRAM-39, or TRAM-7 or 1 μM CLT, ChTX, or ChTX-Glu^{32} as in *B*. The bactericidal activity of 10-μl samples was measured and expressed as described in *B*, relative to secretions released by stimulation with LPS in the absence of IKCa1 inhibitors.

milieu (20, 24, 35). Blockade of mIKCa1 would depolarize the membrane and attenuate the calcium signaling response required to generate a complete Paneth cell secretory response. The mIKCa1 channel may also influence secretion of antimicrobial peptides from other mucosa in the airway, gingival crevice, oropharynx, or urogenital epithelium. The involvement of mIKCa1 in Paneth cell secretion as shown here does not exclude potential roles for other subtypes of calcium-activated K^+ channels in antimicrobial peptide secretion by any of these cells.

CLT is being evaluated in human clinical trials for the treatment of secretory diarrheas due to its ability to block IKCa1 in the colonic epithelium (36, 37). Our finding that highly selective blockers of the IKCa1 channel diminish secretion of Paneth cell antimicrobial peptides in response to bacterial exposure suggests that IKCa1 blockade may have deleterious effects on innate immune mechanisms in the small intestine. To our knowledge, Paneth cell dysfunction has not been identified with human disease. However, in mice genetically defective for the procryptdin-activating metalloproteinase matrily-

nM TRAM-34, 100 nM ChTX-Glu^{32}, 100 nM CLT, and 10 μM TRAM-7 on representative whole-cell IK currents. *G*, pharmacology of mIKCa1. K_d values were determined by testing every compound three times at four concentrations and fitting the Hill equation (n_H) to the reduction of slope conductance at −80 mV. Mean + S.D. are shown. ■, ChTX (K_d = 4 ± 1 nM, n_H = 1.05); △, TRAM-34 (K_d = 21 ± 3 nM, n_H = 1.18); ●, ShK (K_d = 26 ± 3 nM, n_H = 1.08); ○, ChTX-Glu^{32} (K_d = 37 ± 4 nM, n_H = 0.97); ◆, TRAM-39 (K_d = 75 ± 10 nM, n_H = 1.14); ○, CLT (K_d = 80 ± 9 nM, n_H = 1.12); ♦, TRAM-3 (K_d = 490 ± 30 nM, n_H = 1.05); ◇, nifedipine (K_d = 4.2 ± 0.4 μM, n_H = 1.08); ⋆, econazole (K_d = 11 ± 0.9 μM, n_H = 1.1); ▽, TRAM-7 (K_d > 25 μM); ▼, tetraethylammonium (K_d = 28 ± 3 mM, n_H = 1.03).

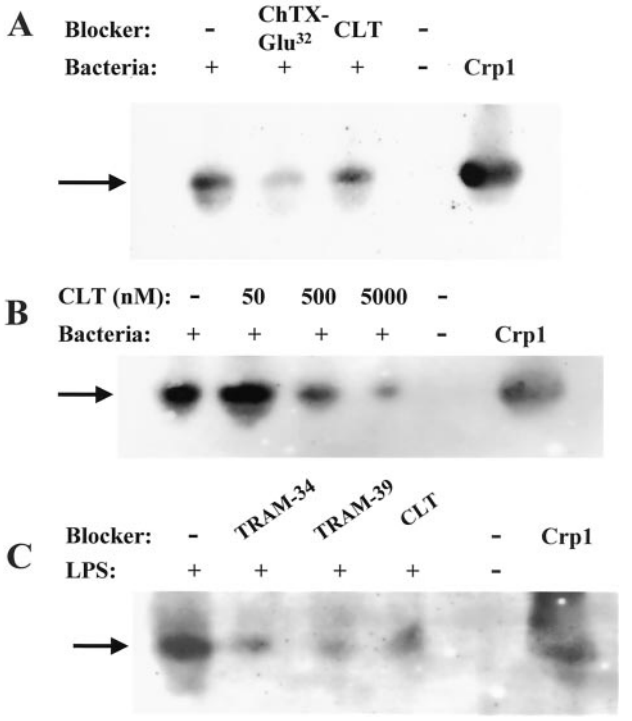

FIG. 5. **Inhibition of cryptdin secretion by selective inhibitors of IKCa1.** Proteins were extracted from secretions collected from crypts incubated with bacteria in the presence or absence of CLT or ChTX-Glu^{32} (Fig. 4*A*), increasing dosages of CLT (Fig. 4*B*), or with 100 ng/ml LPS in the presence of 200 μM TRAM-34, TRAM-39, or 1 μM CLT (Fig. 4*C*). Cryptdins were detected by Western blot analysis following acid-urea PAGE (see "Experimental Procedures" (10), and *arrows* indicate immunoreactive cryptdins in all panels. *Lanes*: *plus characters* denote presence of bacterial or LPS secretory stimuli as noted, and *minus characters* denote absence of a bacterial or LPS secretory stimulus. Similarly, *plus* and *minus characters* denote the respective presence or absence of blockers as noted. *Crp1* denotes lanes containing 1 μg of synthetic cryptdin-1.

sin, the lack of activated intestinal α-defensins correlates with a diminished ability of the mice to clear orally administered enteric infections, and matrilysin-null mice are 10-fold more susceptible to systemic disease caused by *S. typhimurium* infection (27). Defects in mIKCa1 expression or function could adversely affect enteric host defense by attenuating secretory responses to infection and perhaps increasing host susceptibility to bacterial colonization.

Acknowledgments—We thank Seth Alper for his generous gift of the mIKCa1 clone for the electrophysiological experiments and Khoa Nguyen, Hao Truong, and Chialing Wu for excellent technical assistance.

REFERENCES

1. Cociancich, S., Dupont, A., Hegy, G., Lanot, R., Holder, F., Hetru, C., Hoffmann, J. A., and Bulet, P. (1994) *Biochem. J.* **300,** 567–575
2. Borregaard, N., Elsbach, P., Ganz, T., Garred, P., and Svejgaard, A. (2000) *Immunol. Today* **21,** 68–70
3. Ganz, T., and Lehrer, R. I. (1997) *Curr. Opin. Hematol.* **4,** 53–58
4. Ganz, T., Selsted, M. E., Szklarek, D., Harwig, S. S., Daher, K., Bainton, D. F., and Lehrer, R. I. (1985) *J. Clin. Invest.* **76,** 1427–1435
5. Martin, E., Ganz, T., and Lehrer, R. I. (1995) *J. Leukoc. Biol.* **58,** 128–136
6. Schonwetter, B. S., Stolzenberg, E. D., and Zasloff, M. A. (1995) *Science* **267,** 1645–1648
7. Goldman, M. J., Anderson, G. M., Stolzenberg, E. D., Kari, U. P., Zasloff, M., and Wilson, J. M. (1997) *Cell* **88,** 553–560
8. Quayle, A. J., Porter, E. M., Nussbaum, A. A., Wang, Y. M., Brabec, C., Yip, K. P., and Mok, S. C. (1998) *Am. J. Pathol.* **152,** 1247–1258
9. Valore, E. V., Park, C. H., Quayle, A. J., Wiles, K. R., McCray, P. B., Jr., and Ganz, T. (1998) *J. Clin. Invest.* **101,** 1633–1642
10. Ayabe, T., Satchell, D. P., Wilson, C. L., Parks, W. C., Selsted, M. E., and Ouellette, A. J. (2000) *Nat. Immunol.* **1,** 113–138
11. Bals, R., Goldman, M. J., and Wilson, J. M. (1998) *Infect. Immun.* **66,** 1225–1232
12. Bals, R., Wang, X., Wu, Z., Freeman, T., Bafna, V., Zasloff, M., and Wilson, J. M. (1998) *J. Clin. Invest.* **102,** 874–880
13. Diamond, G., and Bevins, C. L. (1998) *Clin. Immunol. Immunopathol.* **88,** 221–225
14. Satoh, Y., Ishikawa, K., Oomori, Y., Takeda, S., and Ono, K. (1992) *Cell Tissue Res.* **269,** 213–220
15. Satoh, Y., Habara, Y., Ono, K., and Kanno, T. (1995) *Gastroenterology* **108,** 1345–1356
16. Ishii, T. M., Silvia, C., Hirschberg, B., Bond, C. T., Adelman, J. P., and Maylie, J. (1997) *Proc. Natl. Acad. Sci. U. S. A.* **94,** 11651–11656
17. Logsdon, N. J., Kang, J., Togo, J. A., Christian, E. P., and Aiyar, J. (1997) *J. Biol. Chem.* **272,** 32723–32726
18. Vandorpe, D. H., Shmukler, B. E., Jiang, L., Lim, B., Maylie, J., Adelman, J. P., de Franceschi, L., Cappellini, M. D., Brugnara, C., and Alper, S. L. (1998) *J. Biol. Chem.* **273,** 21542–21553
19. Joiner, W. J., Wang, L. Y., Tang, M. D., and Kaczmarek, L. K. (1997) *Proc. Natl. Acad. Sci. U. S. A.* **94,** 11013–11018
20. Ghanshani, S., Wulff, H., Miller, M. J., Rohm, H., Neben, A., Gutman, G. A., and Cahalan. (2000) *J. Biol. Chem.* **275,** 37137–37149
21. Fanger, C. M., Ghanshani, S., Logsdon, N. J., Rauer, H., Kalman, K., Zhou, J., Beckingham, K., Chandy, K. G., Cahalan, M. D., and Aiyar, J. (1999) *J. Biol. Chem.* **274,** 5746–5754
22. Wulff, H., Miller, M. J., Haensel, W., Grissmer, S., Cahalan, M. D., and Chandy, K. G. (2000) *Proc. Natl. Acad. Sci. U. S. A.* **97,** 8151–8156
23. Rauer, H., Lanigan, M. D., Pennington, M. W., Aiyar, J., Ghanshani, S., Cahalan, M. D., Norton, R. S., and Chandy, K. G. (2000) *J. Biol. Chem.* **275,** 1201–1208
24. Fanger, C. M., Rauer, H., Neben, A. L., Miller, M. J., Rauer, H., Wulff, H., Rosa, J. C., Ganellin, C. R., Chandy, K. G., and Cahalan, M. D. (2001) *J. Biol. Chem.* **276,** 12249–12256
25. Bjerknes, M., and Cheng, H. (1981) *Anat. Rec.* **199,** 565–574
26. Cano-Gauci, D. F., Lualdi, J. C., Ouellette, A. J., Brady, G., Iscove, N. N., and Buick, R. N. (1993) *Exp. Cell Res.* **208,** 344–349
27. Wilson, C. L., Ouellette, A. J., Satchell, D. P., Ayabe, T., López-Boado, Y. S., Stratman, J. L., Hultgren, S. J., Matrisian, L. M., and Parks, W. C. (1999) *Science* **286,** 113–117
28. Darmoul, D., and Ouellette, A. J. (1996) *Am. J. Physiol.* **271,** G68–G74
29. Darmoul, D., Brown, D., Selsted, M. E., and Ouellette, A. J. (1997) *Am. J. Physiol.* **272,** G197–G206
30. Ghanshani, S., Coleman, M., Gustavsson, P., Wu, A. C., Gargus, J. J., Gutman, G. A., Dahl, N., Mohrenweiser, H., and Chandy, K. G. (1998) *Genomics* **51,** 160–161
31. Rauer, H., Pennington, M., Cahalan, M., and Chandy, K. G. (1999) *J. Biol. Chem.* **274,** 21885–21892
32. Ayub, M., and Levell, M. J. (1990) *Biochem. Pharmacol.* **40,** 1569–1575
33. Maurice, M., Pichard, L., Daujat, M., Fabre, I., Joyeux, H., Domergue, J., and Maurel, P. (1992) *FASEB J.* **6,** 752–758
34. Fowler, S. M., Riley, R. J., Pritchard, M. P., Sutcliffe, M. J., Friedberg, T., and Wolf, R. C. (2000) *Biochemistry* **39,** 4406–4414
35. Cahalan, M. D., and Chandy, K. G. (1997) *Curr. Opin. Biotechnol.* **8,** 749–756
36. Rufo, P. A., Jiang, L., Moe, S. J., Brugnara, C., Alper, S. L., and Lencer, W. I. (1996) *J. Clin. Invest.* **98,** 2066–2075
37. Rufo, P. A., Merlin, D., Riegler, M., Ferguson-Maltzman, M. H., Dickinson, B. L., Brugnara, C., Alper, S. L., and Lencer, W. I. (1997) *J. Clin. Invest.* **100,** 3111–3120